Channel waveguide lasers in Nd:GGG crystals fabricated by femtosecond laser inscription

Chao Zhang,[1] Ningning Dong,[1] Jin Yang,[1] Feng Chen,[1,*] Javier R. Vázquez de Aldana,[2] Qingming Lu[3]

[1]*School of Physics, Key Laboratory of Particle Physics and Particle Irradiation (MOE) and State Key Laboratory of Crystal Materials, Shandong University, Jinan 250100, China*
[2]*Laser Microprocessing Group, Universidad de Salamanca, Salamanca 37008, Spain*
[3] *School of Chemistry and Chemical Engineering, Shandong University, Jinan 250100, China*
[*]*drfchen@sdu.edu.cn*

Abstract: Buried channel waveguides have been fabricated in Nd:GGG crystals by using the femtosecond laser inscription. The waveguides are confined between two filaments with propagation losses of 2.0 dB/cm. Stable continuous wave laser oscillation at ~1061 nm has been demonstrated at room temperature. Under 808 nm optical excitation, a pump threshold of 29 mW and a slope efficiency of 25% have been obtained.

OCIS codes: (230.7380) Waveguides, channeled; (350.3390) Laser materials processing; (149.3380) Laser materials.

References and links

1. D. Kip, "Photorefractive waveguides in oxide crystals: fabrication, properties, and applications," Appl. Phys. B **67**(2), 131–150 (1998).
2. J. I. Mackenzie, "Dielectric solid-state planar waveguide lasers: A Review," IEEE J. Sel. Top. Quantum Electron. **13**(3), 626–637 (2007).
3. G. A. Torchia, A. Rodenas, A. Benayas, E. Cantelar, L. Roso, and D. Jaque, "Highly efficient laser action in femtosecond-written Nd:yttrium aluminum garnet ceramic waveguides," Appl. Phys. Lett. **92**(11), 111103 (2008).
4. Y. Yao, Y. Tan, N. Dong, F. Chen, and A. A. Bettiol, "Continuous wave Nd:YAG channel waveguide laser produced by focused proton beam writing," Opt. Express **18**(24), 24516–24521 (2010).
5. T. Calmano, J. Siebenmorgen, O. Hellmig, K. Petermann, and G. Huber, "Nd:YAG waveguide laser with 1.3 W output power, fabricated by direct femtosecond laser writing," Appl. Phys. B **100**(1), 131–135 (2010).
6. J. Siebenmorgen, T. Calmano, K. Petermann, and G. Huber, "Highly efficient Yb:YAG channel waveguide laser written with a femtosecond-laser," Opt. Express **18**(15), 16035–16041 (2010).
7. T. Calmano, A.-G. Paschke, J. Siebenmorgen, S. T. Fredrich-Thornton, H. Yagi, K. Petermann, and G. Huber, "Characterization of an Yb:YAG ceramic waveguide laser, fabricated by the direct femtosecond-laser writing technique," Appl. Phys. B **103**(1), 1–4 (2011).
8. Y. Tan, F. Chen, J. R. Vázquez de Aldana, G. A. Torchia, A. Benayas, and D. Jaque, "Continuous wave laser generation at 1064 nm in femtosecond laser inscribed Nd:YVO_4 channel waveguides," Appl. Phys. Lett. **97**(3), 031119–031121 (2010).
9. Y. Tan, A. Rodenas, F. Chen, R. R. Thomson, A. K. Kar, D. Jaque, and Q. Lu, "70% slope efficiency from an ultrafast laser-written Nd:$GdVO_4$ channel waveguide laser," Opt. Express **18**(24), 24994–24999 (2010).
10. F. M. Bain, A. A. Lagatsky, R. R. Thomson, N. D. Psaila, N. V. Kuleshov, A. K. Kar, W. Sibbett, and C. T. A. Brown, "Ultrafast laser inscribed Yb:$KGd(WO_4)_2$ and Yb:$KY(WO_4)_2$ channel waveguide lasers," Opt. Express **17**(25), 22417–22422 (2009).
11. M. Pollnau, C. Grivas, L. Laversenne, J. S. Wilkinson, R. W. Eason, and D. P. Shepherd, "Ti:Sapphire waveguide lasers," Laser Phys. Lett. **4**(8), 560–571 (2007).
12. N. V. Baburin, B. I. Galagan, Y. K. Danileiko, N. N. Il'ichev, A. V. Masalov, V. Y. Molchanov, and V. A. Chikov, "Two-frequency mode-locked lasing in a monoblock diode-pumped Nd^{3+}:GGG laser," IEEE Quant. Electron. **31**(4), 303–304 (2001).
13. Z. Jia, X. Tao, C. Dong, X. Cheng, W. Zhang, F. Xu, and M. Jiang, "Study on crystal growth of large size Nd^{3+}:$Gd_3Ga_5O_{12}$ (Nd^{3+}:GGG) by Czochralski method," J. Cryst. Growth **292**(2), 386–390 (2006).
14. L. J. Qin, D. Y. Tang, G. Q. Xie, C. M. Dong, Z. T. Jia, and X. T. Tao, "High-power continuous wave and passively Q-switched laser operations of a Nd:GGG crystal," Laser Phys. Lett. **5**(2), 100–103 (2008).
15. F. Chen, "Construction of two-dimensional waveguides in insulating optical materials by means of ion beam implantation for photonic applications: Fabrication methods and research progress," Crit. Rev. Solid State Mater. Sci. **33**(3), 165–182 (2008).

#146970 - $15.00 USD Received 4 May 2011; revised 2 Jun 2011; accepted 7 Jun 2011; published 13 Jun 2011

16. F. Chen, X. L. Wang, and K. M. Wang, "Development of ion-implanted optical waveguides in optical materials: A review," Opt. Mater. **29**(11), 1523–1542 (2007).
17. S. J. Field, D. C. Hanna, A. C. Large, D. P. Shepherd, A. C. Tropper, P. J. Chandler, P. D. Townsend, and L. Zhang, "Ion-implanted Nd:GGG channel waveguide laser," Opt. Lett. **17**(1), 52–54 (1992).
18. Y. Ren, N. Dong, Y. Tan, J. Guan, F. Chen, and Q. Lu, "Continuous Wave Laser Generation in Proton Implanted Nd:GGG Planar Waveguides," J. Lightwave Technol. **28**, 3578–3581 (2010).
19. R. R. Gattass and E. Mazur, "Femtosecond laser micromachining in transparent materials," Nat. Photonics **2**(4), 219–225 (2008).
20. S. Juodkazis, V. Mizeikis, and H. Misawa, "Three-dimensional microfabrication of materials by femtosecond lasers for photonics applications," J. Appl. Phys. **106**(5), 051101, 05111–05114 (2009).
21. M. Ams, G. D. Marshall, P. Dekker, J. A. Piper, and M. J. Withford, "Ultrafast laser written active devices," Laser Photon. Rev. **3**(6), 535–544 (2009).
22. F. Fusari, R. R. Thomson, G. Jose, F. M. Bain, A. A. Lagatsky, N. D. Psaila, A. K. Kar, A. Jha, W. Sibbett, and C. T. A. Brown, "Lasing action at around 1.9 μm from an ultrafast laser inscribed Tm-doped glass waveguide," Opt. Lett. **36**(9), 1566–1568 (2011).
23. K. M. Davis, K. Miura, N. Sugimoto, and K. Hirao, "Writing waveguides in glass with a femtosecond laser," Opt. Lett. **21**(21), 1729–1731 (1996).
24. R. Regener and W. Sohler, "Loss in low-finesse Ti:$LiNbO_3$ optical waveguide resonators," Appl. Phys. B **36**(3), 143–147 (1985).
25. J. Siebenmorgen, K. Petermann, G. Huber, K. Rademaker, S. Nolte, and A. Tunnermann, "Femtosecond laser written stress-induced Nd:$Y_3Al_5O_{12}$ (Nd:YAG) channel waveguide laser," Appl. Phys. B **97**(2), 251–255 (2009).
26. J. Burghoff, H. Hartung, S. Nolte, and A. Tunnermann, "Structural properties of femtosecond laser-induced modifications in $LiNbO_3$," Appl. Phys., A Mater. Sci. Process. **86**(2), 165–170 (2006).
27. I. Mansour and F. Caccavale, "An improved procedure to calculate the refractive index profile from the measured near-field intensity," J. Lightwave Technol. **14**(3), 423–428 (1996).
28. G. A. Torchia, P. F. Meilán, A. Rodenas, D. Jaque, C. Mendez, and L. Roso, "Femtosecond laser written surface waveguides fabricated in Nd:YAG ceramics," Opt. Express **15**(20), 13266–13271 (2007).
29. B. Poumellec, L. Sudrie, M. Franco, B. Prade, and A. Mysyrowicz, "Femtosecond laser irradiation stress induced in pure silica," Opt. Express **11**(9), 1070–1079 (2003).
30. D. Jaque, U. Caldiño, J. J. Romero, and J. García Solé, "Influence of Nd concentration on continuous wave laser properties of $Ca_3Ga_2Ge_3O_{12}$:Nd^{3+} laser garnet crystal," J. Appl. Phys. **86**, 6617–6623 (1999).
31. J. J. Romero, D. Jaque, U. Caldiño, G. Boulon, Y. Guyot, and J. García Solé, "Stimulated emission, excited state absorption and laser performance optimization of the Nd^{3+}: $Ca_3Ga_2Ge_3O_{12}$ laser system," J. Appl. Phys. **91**, 1754–1760 (2002).

1. Introduction

Optical waveguide structures are basic elements in integrated photonics and modern optical communication systems. Such structures could confine light in very small volumes with dimensions of the order of several micrometers, in which much high optical intensity could be achieved with respect to the bulks [1]. Owing to this advantage, some performances of the bulk materials may be considerably enhanced in waveguide structures. Particularly, waveguide lasers could be more efficient than bulk lasers due to the confinement induced improvement in spatial overlaps between pump and laser beams [2]. Crystalline waveguide lasers have been realized in a couple of gain materials, e.g., Nd or Yb doped YAG [3–7], Nd doped YVO_4 or $GdVO_4$ [8,9], Yb doped KYW or KGW [10] and Ti:Al_2O_3 [11]. Nd:GGG (Nd:$Gd_3Ga_5O_{12}$, neodymium doped gadolinium gallium garnet) is one of the most excellent gain media for solid state lasers [12–14]. Because of its very stable chemical properties, normal chemical methods, such as metal ion thermal in-diffusion, ion exchange, cannot be applied to Nd:GGG for waveguide fabrication. Therefore, physical techniques, such as ion implantation [15,16], could be more suitable for waveguide fabrication. Waveguides have been fabricated in Nd:GGG crystal by using H or He ion implantation, and the correlated waveguide lasers was realized [17,18]. Ultrafast laser inscription (using femtosecond, fs, pulses) has emerged to be a powerful technique for three-dimensional volume microstructuring of dielectric materials [19,20]. In recent years, active waveguides in different crystals and glasses have been produced by pulsed fs-laser writing through the stress-induced mechanisms, and efficient waveguide lasers have been generated in some of these samples [5–11,21–23]. Up to now, the fs-laser writing has not been applied to Nd:GGG crystals for waveguide construction. In this work, we report, to our knowledge for the first time, on the fabrication of channel waveguides in Nd:GGG crystals by

#146970 - $15.00 USD Received 4 May 2011; revised 2 Jun 2011; accepted 7 Jun 2011; published 13 Jun 2011

using femtosecond (fs) laser inscription and the room-temperature continuous wave (cw) laser generation in the formed structures.

2. Experiments

The Nd:GGG crystal (doped by 1 at. % Nd^{3+} ions) was cut with the size of 10×4×1.5 mm^3, and all its faces were polished up to optical quality. The buried waveguides were fabricated under the "double-line" configuration by using a Ti:Sapphire laser system, which delivered 120 fs pulses, linearly polarized at 796 nm and with a repetition rate of 1 kHz. The laser beam was focus by a 20× microscope objective (N.A=0.4), and the sample was located at a XYZ motorized stage with a spatial resolution of 0.2 μm. The linear focus of the objective was located 150 μm beneath the surface of the crystal and the pulse energy was set to 5.8 μJ. Under these conditions, two filaments were written separated by 15 μm by scanning the piece at a translation velocity of 25 μm/s. Propagation losses of the waveguides as low as 2dB/cm were measured by using the Fabry-Perot resource method at wavelength of 632.8 nm based on an endface coupling arrangement [24]. During the measurement, the sample was slightly heated, generating a temperature increment of 5°C, which resulted in the periodically oscillations of the output light power.

The waveguide laser experiments were performed by using an end face pumping system. A cw Ti:Sapphire laser (Coherent MBR 110, tunable range between 700 and 970 nm) generated a pump light beam at wavelength of 808 nm. A convex lens (with focus length of 25 mm) was used to focus the pump light beam into the channel waveguide, and the laser oscillations from the waveguide were collected by a 20× microscope objective lens (N.A = 0.4). We used two mirrors as the resonant cavity for waveguide laser generation. The input mirror (with the transmission of 98% at 808 nm and reflectivity > 99% at 1064 nm) was attached at the input face of the waveguide, and another mirror, which has reflectivity >99% at 808 nm and 95% at 1064 nm, was attached at the exit face of the waveguide. We used a CCD camera to obtain the output images (modal profiles) of the waveguide laser. The input and output beam powers were measured by the powermeter. A spectrometer (with resolution of 0.2 nm) was utilized to analyze the emission spectra (laser intensity vs. wavelength curves) of the laser beams from the waveguide.

3. Results and discussion

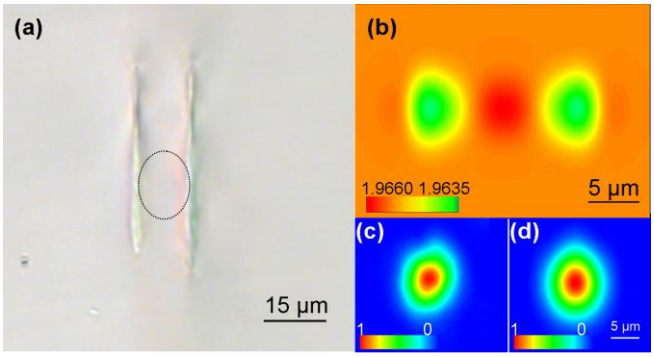

Fig. 1. (a) Optical transmission microphotograph of the "double-filament" Nd:GGG waveguide. (b) Refractive index profile at the cross section of the Nd:GGG channel waveguide. (c) Measured near field-intensity distribution of the fundamental mode TM_{00} at 632.8 nm. (d) Calculated modal profile of the fundamental mode TM_{00}.

Figure 1(a) shows the microscopic photograph of the cross section of the waveguide sample taken under transmission illumination. As one can see, there are two lines (filaments) with separation of 15μm, representing the tracks of the fs writing (the pulse propagated from top to bottom). The waveguide is located between these two filaments. The refractive index

#146970 - $15.00 USD Received 4 May 2011; revised 2 Jun 2011; accepted 7 Jun 2011; published 13 Jun 2011

distributions of the waveguide cross section cannot be directly measured by the *m*-line technique, which has been widely applied for index measurement of planar waveguide. In order to construct a 2D refractive index profile of the Nd:GGG channel waveguide, we first assumed that the distribution is a step-like one. By the measurement of N.A. of the waveguide, we obtained the maximum value of refractive index changes of the waveguide, which could be roughly estimated by measuring the N.A. of the waveguides, using the formula

$$\Delta n = \frac{\sin^2 \Theta_m}{n} \tag{1}$$

where Θ_m is the maximum incident angular deflection at which no transmitted power change is occurring, while n is the refractive index of the substrate [25]. Figure 1(b) shows the reconstructed 2D refractive index profile at the cross section. As one can see, a positive index change $\Delta n_w \approx +6\times10^{-4}$ appears in the waveguide core due to the induced stress [28]; whilst in the two filaments, there is a refractive index decrease of $\Delta n_f \approx -1.9\times10^{-3}$. Based on this reconstructed index profile, we calculated the modal profile of the waveguide [Fig. 1(d)] which is made by using the finite-difference beam propagation method (FD-BPM) with the software Rsoft® [26,27]. Figure 1(c) show the near field intensity image (modal profile of TM_{00} mode) from the Nd:GGG waveguide at the wavelength of 632.8 nm. By comparing Figs. 1(c) and (d), one can conclude that the calculated modal profile is in good agreement with the experimental result, which, in turn, suggests the reasonability of the refractive index construction.

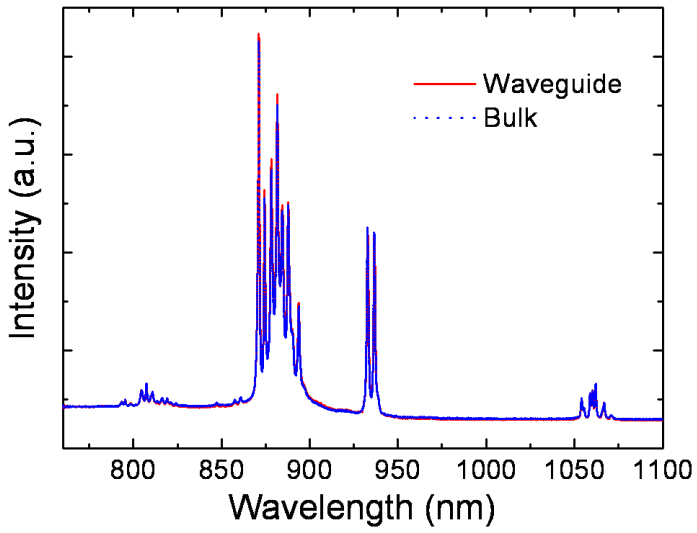

Fig. 2. Room temperature micro-luminescence spectra comparison of Nd^{3+} ions from the channel waveguide (red solid line) and bulk (blue dotted line) of the Nd:GGG sample, respectively

Figure 2 depicts the comparison of the micro-luminescence emission spectra of Nd^{3+} obtained from the waveguide and from the Nd:GGG bulk at room temperature. As one can see, the spectra obtained in the waveguides are of high resemblance to those in the bulk of the crystal, for both spectral distribution and intensity. This means that the original fluorescence properties are well preserved in the waveguide volume compared with those of the bulk, which is an advantage for potential laser application of the Nd:GGG crystal system.

#146970 - $15.00 USD Received 4 May 2011; revised 2 Jun 2011; accepted 7 Jun 2011; published 13 Jun 2011

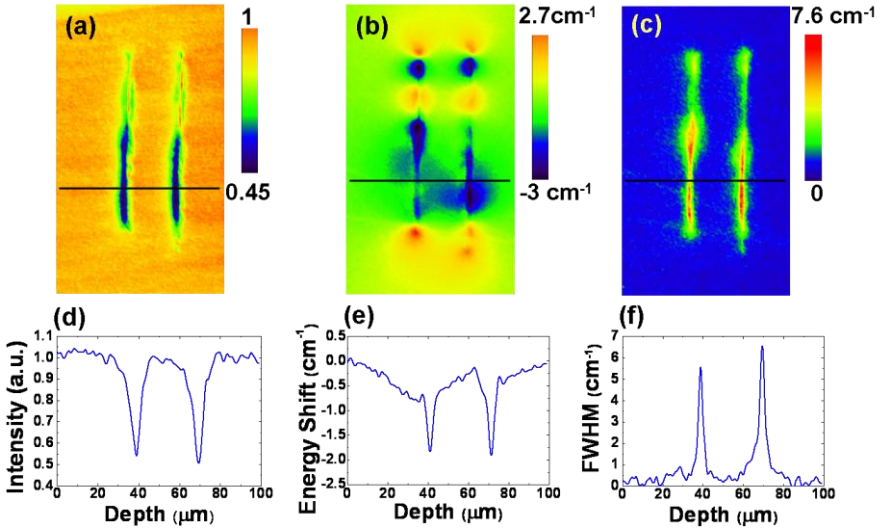

Fig. 3. Spatial distribution of the (a) emitted intensity, (b) energy shift and (c) FWHM of the $^4F_{3/2}\rightarrow{}^4I_{9/2}$ Nd^{3+} emission line around 933 nm obtained from the end face of the waveguide. (d), (e) and (f) are the corresponding 1D profile of the selected black lines in the above pictures, respectively.

In order to obtain a better understanding of the physical mechanism at the basis of the femtosecond laser written waveguide formation in Nd:GGG crystal, we measured the spatial distribution of the integrated intensity (Fig. 3(a)), spectral shift (Fig. 3(b)) and bandwidth (Fig. 3(c)) of the 933 nm Nd^{3+} emission line over the waveguide's cross section [28,29]. At the purpose of give a clear description, we show the 1D linear profiles as obtained along the black lines. As we can see from Figs. 3 (a) and (d), it is evident that there is a clear fluorescence quenching in the filaments while the photoluminescence properties are well preserved in the waveguide volumes with respect to the bulk of the crystal, which is of high consistence with the result of Fig. 2. At the same time, there is a relevant line-width increase at the filaments, as shown in Figs. 3 (c) and (f). Both intensity reduction and FWHM increase at the filaments are aroused by the lattice defects and disorder induced during the writing process, respectively. Figures 3(b) and 3(e) clearly display that the 933 nm emission line shifts to lower energies at the damage tracks and the waveguide volume delimited by the two filaments, whereas it suffers a blue shift at the front and the end of the filaments (top and bottom of the filaments in the picture) which, in a first approximation, correspond to compressive and expansive stress, respectively. Such results suggest that different structural modification mechanisms have been induced at the filaments and their surrounding areas. Indeed similar density fluctuations have been observed in Nd:YAG [29].

Figure 4(a) depicts the measured emission spectrum around 1061 nm from the Nd:GGG channel waveguide when it was optically excited close to threshold. The emission line was centered at 1060.7 nm with a FWHM of ~0.4 nm, clearly denoting a laser oscillation line, which is relevant to the $^4F_{3/2}\rightarrow{}^4I_{11/2}$ fluorescence band of Nd^{3+} ions [30,31]. The inset shows the image of the output light beam at 1061 nm, when the pumping power was above the oscillation threshold. Figure 4(b) depicts the output power (at wavelength of ~1061 nm) generated in the Nd:GGG waveguide as a function of the 808 nm absorbed power. From the linear (solid line) fit of the experimental data (dots), one can determine that the power threshold (P_{th}) for a laser oscillation is 29 mW. This value is higher than that of the He ion implanted Nd:GGG channel waveguide laser [17], which may be partly due to the relatively higher propagation loss of the fs-laser written sample. In addition, a slope coefficient (Φ) of ~25% can be extracted for the waveguide laser system in Nd:GGG sample. The achieved maximum power of the laser at 1061

#146970 - $15.00 USD Received 4 May 2011; revised 2 Jun 2011; accepted 7 Jun 2011; published 13 Jun 2011

nm was ~11 mW for the maximum absorbed pump power of ~70 mW, denoting an optical conversion efficiency of 15.7%.

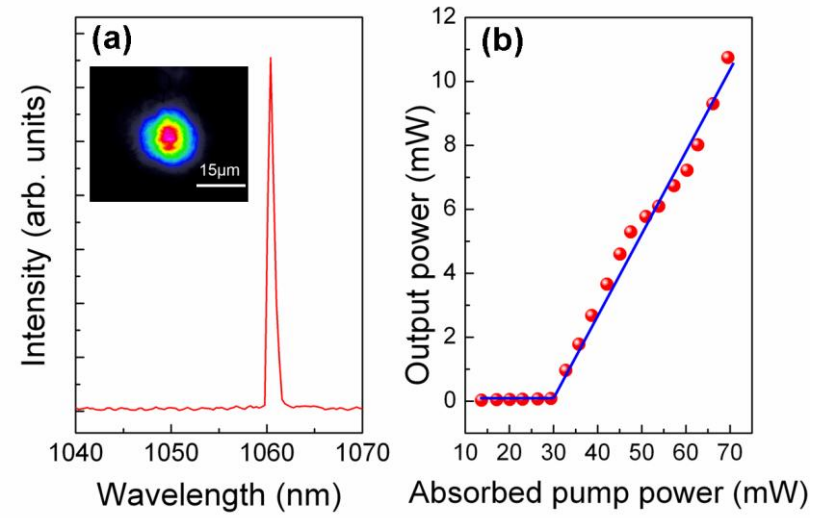

Fig. 4. (a) The cw laser oscillation spectrum obtained from Nd:GGG waveguide with optical pumping at 808 nm. The inset shows the intensity distribution of the output light at 1061 nm. (b) The cw waveguide laser output power at 1061 nm as a function of absorbed pump power at 808 nm. The threshold is 29 mW, and the slope efficiency is 25%.

4. Summary

We have demonstrated the fabrication of channel waveguides in Nd:GGG crystals by using the femtosecond laser inscription "double-line" technique. The good quality near field intensity beam profile of the coupled mode and the absence of any relevant deterioration in the fluorescence properties of Nd ions at the waveguide volume, indicated well guiding prosperities. Stable cw laser oscillation at 1061 nm from Nd:GGG channel waveguide has been observed at room temperature, with an optical pump threshold of 29 mW at 808 nm and a slope efficiency of 25%. The results show a potential application of the fs-laser inscribed Nd:GGG waveguides as integrated light sources.

Acknowledgments

This work is supported by the National Natural Science Foundation of China (Grant No. 10925524), the Promotive Research Fund for Excellent Young and Middle-aged Scientists of Shandong Province, China (Grant No. BS2009CL003), Spanish Ministerio de Ciencia e Innovación through the Consolider Program SAUUL (CSD2007-00013) and Research project FIS2009-09522 and by CONICET (under project PIP 11220090100394). We also acknowledge support from the Centro de Laseres Pulsados CLPU, Salamanca, Spain.

#146970 - $15.00 USD Received 4 May 2011; revised 2 Jun 2011; accepted 7 Jun 2011; published 13 Jun 2011